ISSN. 1412-4785; e-ISSN. 2252-620X, Accredited by Kemendikbudristek No. 105/E/KPT/2022
DOI: 10.17529/jre.v21i2.41353

Design of Deep Learning-Based Pressure Injury Stage Classification Device

Wahmisari Priharti*, Husneni Mukhtar, I Made Prastha Giriwara,
I Made Andi Majesta, and Wayan Abin Bena Bimantara
School of Electrical Engineering, Telkom University
Jl. Telekomunikasi, Terusan Buah Batu, Bandung, Indonesia 40256
*e-mail: wpriharti@telkomuniversity.ac.id

Abstract—**Pressure injury or pressure ulcers could occur due to continuous pressure on the bony prominence of the skin and tissue. Geriatric patients, especially those with limited mobility and several comorbidities, are more susceptible to pressure injury. Stage classification of pressure injury is currently carried out qualitatively and requires clear communication with the patient. This is often not possible in elderly patients due to a lack of perception of pain, causing late detection of pressure injury until they have reached a severe level, and can endanger the patient's life. This study proposes a non-contact device in the form of a camera integrated with a convolutional neural network (CNN) model with MobileNet architecture to classify the level of pressure injury. Testing showed a classification accuracy of 83.3% with an average classification duration of 2.24 s. This aiding device is considered to have great potential to improve faster and more accurate pressure injury assessment in clinical settings.**

Keywords: ***convolutional neural network, elderly, pressure injury, mobilenet, non-contact device***

I. Introduction

Pressure injury or pressure ulcers, also termed decubitus ulcers, are specific injuries to the skin and soft tissue caused by prolonged pressure or shear force on certain parts of the body, usually on bony prominences [1]. The development of these ulcers is a complex process influenced by various external and internal factors, but the main reason is impaired mobility. Conditions that can limit mobility include joint and bone problems, nerve disorders, cardiovascular disease, respiratory disorders, and serious medical conditions that force the patient to stay in bed [2].

Pressure ulcers, combined with an underlying illness, can worsen health and lead to complications like infections, prolonged hospital stays, and more medical costs due to necessary treatments and tests. Additionally, failure to address this problem can heighten the likelihood of mortality [3]. Hospitals have consequently intensified their efforts to diminish pressure ulcers, especially in decubitus and critical patients [4]. However, despite considerable investments in healthcare expenses and preventive measures in nursing, pressure ulcers persist as a significant medical challenge.

Personal factors such as age, nutrition, and health conditions can also worsen the risk of pressure ulcers. Individuals with decreased perception, such as the elderly (> 60 years old), also have a high risk of pressure ulcers occurring since they often do not feel the need to reduce pressure on a particular area [5]-[7]. This is supported by the data from the Global Burden of Disease Study, which revealed that the highest occurrence of pressure ulcers was observed in the 80-84 and 85-89 age groups [8]. From this study, it is apparent that the rate of prevalence rises notably as people get older, especially in females who are more susceptible than males starting from more than 75 years old age group.

Pressure ulcers are classified and described by a staging system that outlines the severity of tissue damage and the visible characteristics of injuries from pressure and/or shear. The widely adopted international staging system is defined by the National Pressure Ulcer Advisory Panel (NPUAP). In 2016, NPUAP published a new terminology of pressure injury to replace pressure ulcer, hence also changing the organization's name to National Pressure Injury Advisory Panel (NPIAP). This change is made to better describe all forms of tissue damage, including early stages of pre-skin breakdown.

The stage of pressure injury defined by NPIAP is classified into four levels, ranging from stage 1, indicating non-blanchable erythema of intact skin, to stage 4 involving full-thickness skin loss with damage to muscle or bone [9]. The stages, images, and characteristics are described in more detail in Table 1.

This staging classification is important because it determines the type and intensity of treatment that should be given. The Braden Scale, developed by Bergstrom in 1978, is used to qualitatively assess the risk of pressure injury based on six risk factors, namely (i) sensory

Received 19 Jan. 2025; Revised 23 May 2025; Accepted 2 June 2025

Table 1. The classification of pressure injury by NPIAP [8]

Stage	Image	Characteristics
1	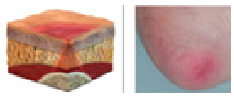	Intact skin with non-blanchable redness of a localized area usually over a bony prominence
2	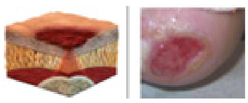	Partial thickness loss of dermis presenting as a shallow, open wound with a red, pink wound bed, without slough.
3	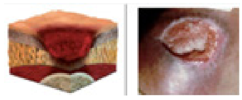	Full-thickness tissue loss. Subcutaneous fat may be visible, but bone, tendon, or muscle are not exposed.
4	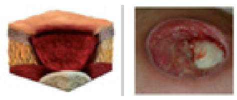	Full thickness tissue loss with exposed bone, tendon, or muscle.

Table 2. Current study of the stage classification of pressure injury

Reference	Methods	Type	Results
[13]	Color sensor	Hardware	The device could classify pressure injury with 85% accuracy, 86.4% precision, 85% recall, and 85.7% F-score.
[14]	Support Vector Machines and GrabCut	Software	The model could classify pressure injury with 96% accuracy, 94% sensitivity, and 94% precision.
[15]	Numerical analysis and imaging	Software	This study proves that the sensitivity and specificity values could affect the classification results.
[16]	Convolutional neural network (CNN)	Software	The accuracy of this study in classifying 121 images of pressure injury is 92.6% and 93,0% with image segmentation.
[17]	Convolutional neural network (CNN)	Software	The classification precision is 87%.
[18]	Statistical colour models	Software	The classification accuracy is less than 80%

perception, (ii) mobility, (iii) moisture, (iv) nutrition, (v) activity, and (vi) friction and shear [10]. However, quantitative assessment of pressure injury is still rare. Studies have shown that physicians who are not skilled in assessing pressure injury often experience difficulties with assessment accuracy, varying between 23% and 58% [11]. Assessment tools such as the NE1 Wound Assessment Tool and the Pressure Ulcer Scale for Healing (PUSH) tool still require direct measurement of the wound, which is time-consuming and does not always provide efficient results [12].

Initial study using color sensors to detect pressure injury in the elderly showed an accuracy of around 85%. This method uses color sensors to measure changes in skin color and identify pressure injury based on color differences [13]. However, this method is quite impractical

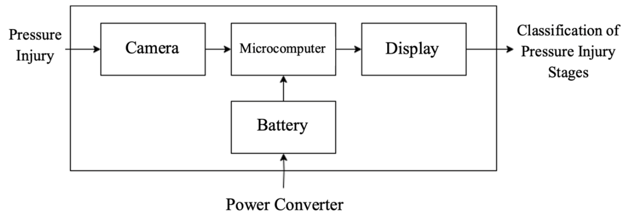

Figure 1. System block diagram

since the injury images need to be captured using a separate device then the analysis could only be done indirectly from the captured injury images. The injury images need to be taken beforehand since direct contact with the injury is not possible, and it could also create inconvenience, hurt, or harm the subject.

Several other studies regarding pressure injury classification, both using hardware or software, were described in Table 2. Most of the studies only produced a pressure injury stage classification algorithm without a specialized image-capturing device. Hence, the quality of the obtained image could vary and affect the classification results.

Therefore, the objective of this study is to design a contactless device that can directly capture and quantitatively classify pressure injury into four stages using the CNN model with the MobileNet architecture. This architecture has advantages in terms of computational efficiency and memory usage, which allows implementation on devices with limited resources. This model is expected to provide a faster and more accurate diagnosis, as well as assist health personnel or paramedics in planning more effective care for patients with pressure injury.

II. Methods

A. *Hardware Design and Components*

The design of the system includes several main components: the image capturing module (camera), a microcomputer that stores the image classification algorithm, the display unit, and the battery as the power supply system. The system block diagrams in Figure 1 show the overall system workflow.

The components were selected based on several performance criteria such as resolution, processing capabilities, and power. The details of components used in this system, along with their specifications and selection justification, are listed in Table 3. The wiring schematics of the components are shown in Figure 2.

The device was designed to be portable and easily used using one hand. The dimension of the device is only 7.5×9.5×19.5 cm^3 with the weight of 420 g, or equivalent to the weight of a regular smartphone and lighter than a common DSLR camera. This device is also equipped with a large display (420×320 resolution LCD) to show the classification results directly during measurement. The anatomy, front and side view design of the device is shown in Figure 3.

During the pressure injury measurement, the user can

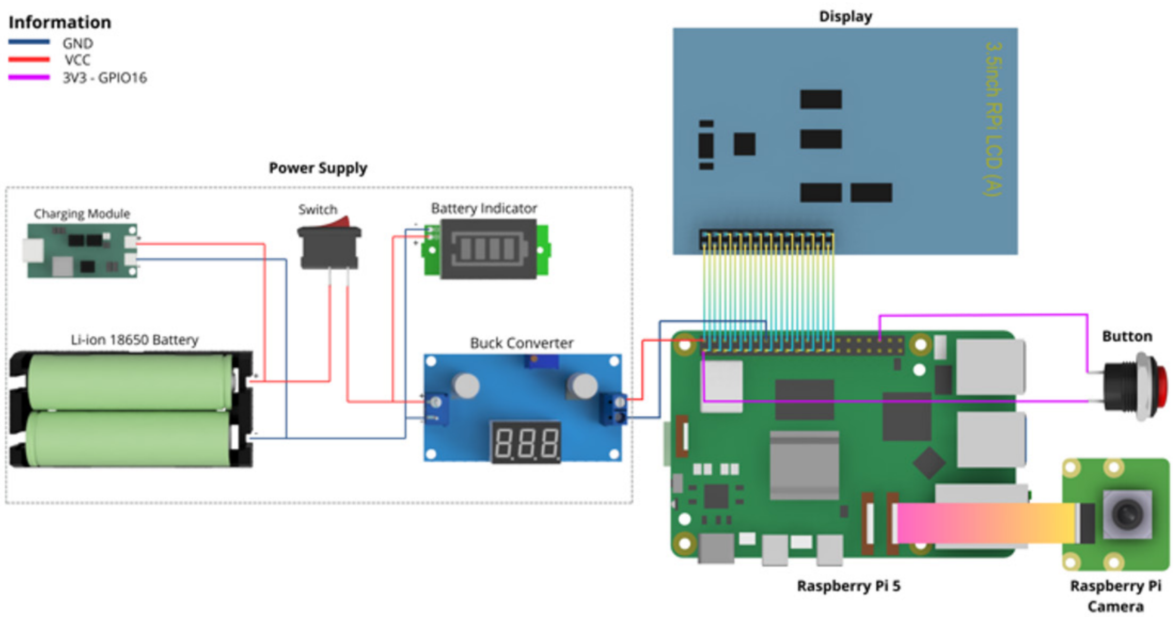

Figure 2. Wiring schematics of the components

Table 3. List of components

Components	Specification	Selection Justification
Camera	Raspberry Pi Cam V3 (4608 × 2592 pixels resolution)	High resolution
Classification Model	Model_V1 TFLite	Compatibility with the device
Microcomputer	Raspberry Pi 5	High CPU speed
Power supply	Li-Ion 18650 battery (3400 mAh), buck converter, charger BMS	Provides stable power
User Interface	Tkinter	Provides simple interface
Input Device	Digital Input Device Button (gpiozero)	Easy to capture images
Memory	SanDisk SD Card 32GB (local storage)	Save images on a timestamp basis

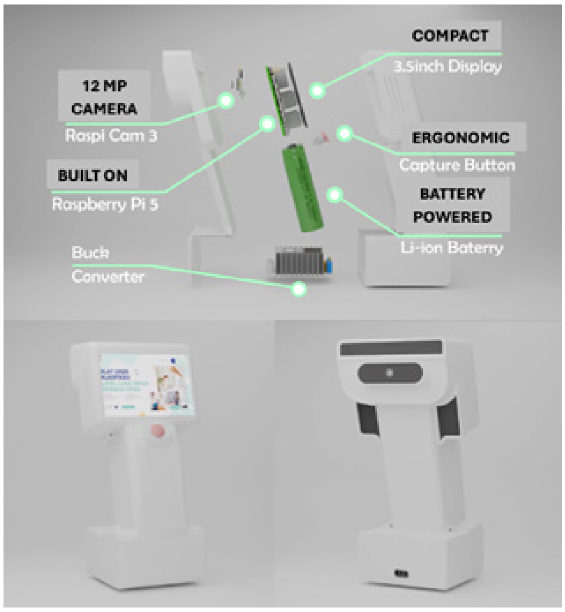

Figure 3. Device anatomy, front and side view

trigger the switch button to turn on the device. The camera module captures images of pressure injury by the press of the digital input device button, which is then processed by the Raspberry Pi 5 using a classification algorithm. The classification results are then displayed on the screen to be accessed and read by the user. The overall workflow diagram of this device is shown in the flowchart in Figure 4.

B. Model Architecture

The proposed model used in this study is a convolutional neural network (CNN) with the MobileNet architecture. CNN is a type of neural network specifically designed to work with image or grid data. CNN uses convolutional layers to extract features from images by applying filters (kernels) to small parts of the image. The basic architecture of CNN consists of several main layers, illustrated in Figure 5 [19].

Deep learning-based methods, such as Mask-R-CNN, showed a classification accuracy of 92.6% and a segmentation accuracy of 93.0% [20]. However, Mask-R-CNN requires a CNN to be used for feature extraction and segmentation of pressure injury images, offering improved accuracy over traditional methods. Another study integrating 3D models for non-invasive assessment showed a precision of 87% [21].

Despite the higher accuracy reported using Mask R-CNN, our proposed CNN-based approach has several important benefits, including ease of use, speed, and deployment viability. Our lightweight architecture enables real-time inference on a low-cost device, which makes it especially appropriate for field use in healthcare settings. This contrasts with Mask R-CNN, which necessitates high computational resources and longer training times.

As illustrated in Figure 5, the simplest CNN

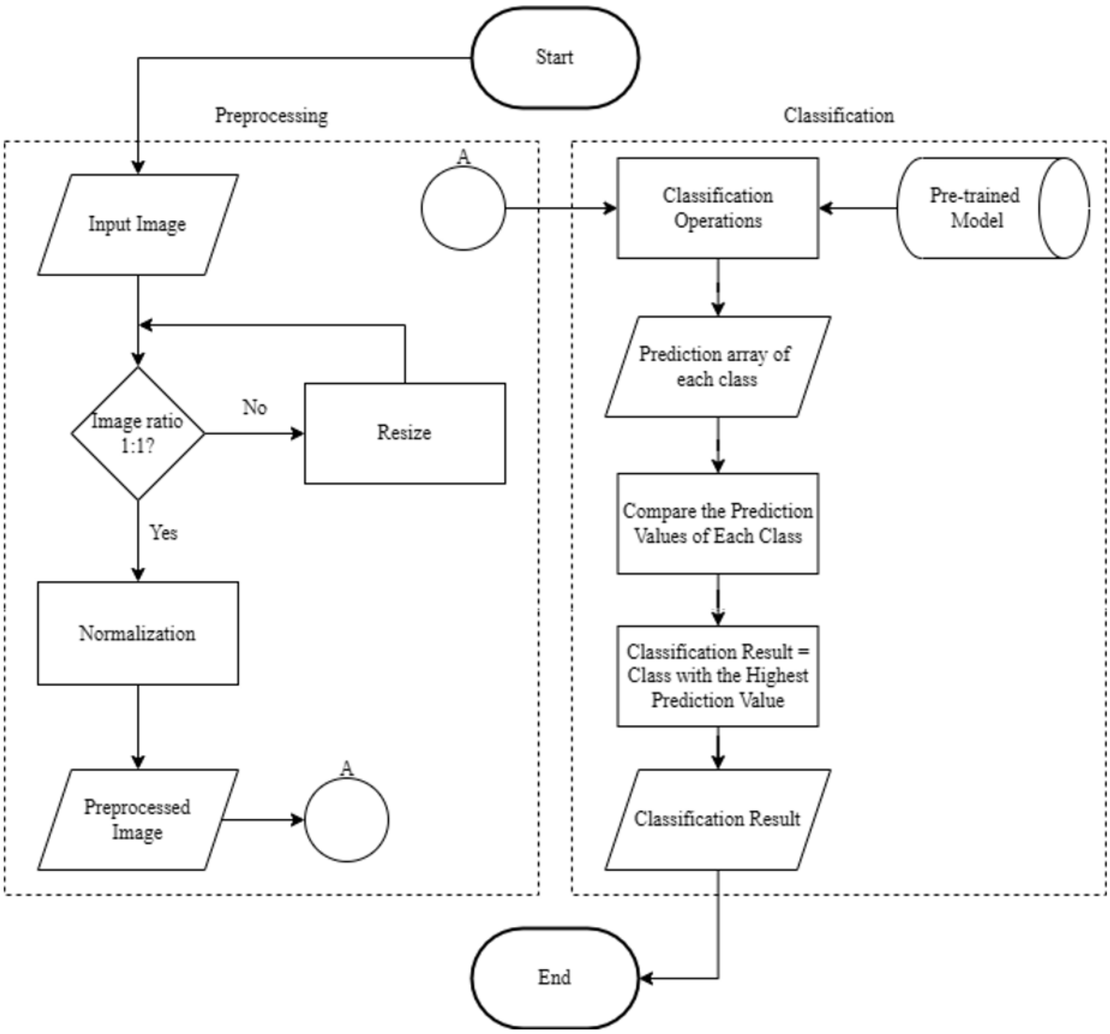

Figure 4. System overall workflow

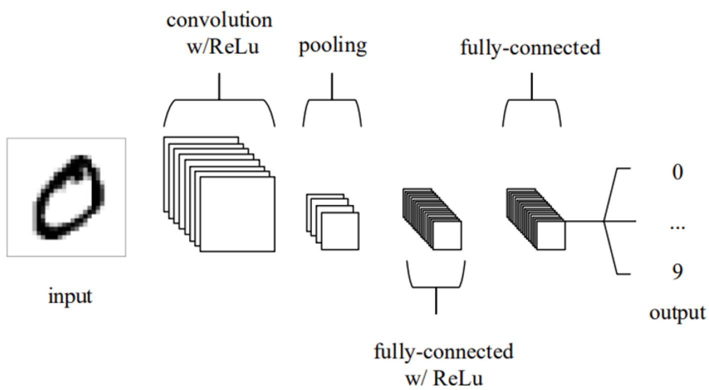

Figure 5. Simple architecture of CNN

architecture starts with the input layer, which receives the raw image and passes it to the convolution layer. The convolutional layer captures local features of the image with a convolution filter. In this layer, the dimension of the feature will be reduced by selecting the maximum or average value in a certain area, which reduces the size of the data and computing. A fully connected layer will connect neurons from the previous layer to the neurons in the final layer. And finally, before the model gives the output, there is a softmax layer which provides a decimal probability for each class. The decimal probability is between 0 and 1 (0 -100%).

MobileNet was chosen as the architecture based on its efficiency in image processing and its ability to provide good accuracy with a relatively small model size [22], [23]. The classification model architecture of this system using MobileNet is shown in Figure 6.

C. Model Datasets and Training

The datasets used in this study were a collection of 2,811 original medical images of pressure injuries

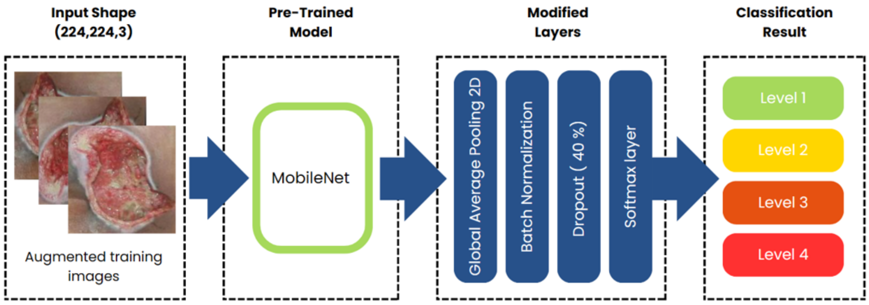

Figure 6. System model classification architecture using MobileNet

Table 4. Image allocation for data training, validation, and testing

Stages	Number of data (images)		
	Training	Validation	Testing
Stage 1	315	90	45
Stage 2	427	122	61
Stage 3	385	110	55
Stage 4	315	90	45
Total	1442	412	206

obtained from Roboflow [24], consisting of four severity stages: stage 1, stage 2, stage 3, and stage 4. These datasets have been labeled with relevant classes (stage 1 to stage 4) and validated by a medical doctor specialized in pressure injury care. From this collection, a subset of 2,059 images was selected and partitioned into training (70%, 1,442 images), validation (20%, 411 images), and test (10%, 206 images) sets. The detailed amount of allocated image for each dataset are described in Table 4.

The dataset source uses different devices to capture the images, such as a Raspberry Pi Camera, a web camera, or even a DSLR. These differences lead to several variations in the resolutions, color profile, image distortion, noise, and artifacts. Hence, to reduce the variance of the datasets across several devices, normalization and alignment of the data were conducted via image pre-processing. The pre-processing stages were done sequentially to ensure that clean and standardized input images are produced, suitable for accurate and reliable classification by the CNN model, which include:

- Aspect ratio verification: The first preprocessing step involves verifying the aspect ratio of the input images. The classification model was trained using square images with a 1:1 aspect ratio; therefore, input images must conform to this format. If the acquired image does not meet this requirement, it is adjusted accordingly to form a square by resizing the dimensions while maintaining image integrity.
- Image resizing: After aspect ratio correction, the image is resized to match the input dimensions required by the convolutional neural network (CNN). In this study, a fixed input size (e.g., 224×224 pixels) is used. Resizing is performed through iterative pixel interpolation algorithms to preserve essential image features during the transformation process.
- Pixel value normalization: Once the image has been resized, pixel value normalization is applied. Originally ranging from 0 to 255 (8-bit format), pixel intensities are rescaled to a range between 0 and 1. This normalization ensures uniform data distribution and improves the stability and convergence speed of the model during inference.

Once all these steps are done, the processed image then becomes an input value for the model to produce the classification result. Then, to increase the diversity of the training dataset and prevent overfitting by creating additional image variations, the data augmentation was applied. The augmentation techniques used include:

- Rotation: Images are rotated in an angle range of -30 to 30 degrees to simulate orientation variations.
- Flipping: The image is flipped horizontally to introduce variations in the image orientation.
- Zooming: Images are zoomed in or out to simulate changes in the shooting distance.
- Shearing: Shearing transforms are applied to create an image distortion effect.
- Brightness Adjustment: The brightness of the image is changed to simulate various lighting conditions.

The initial augmentation phase expanded the training set to 3,370 images through basic transformations such as horizontal flipping and slight rotations. Subsequently, advanced augmentation techniques—including brightness adjustment, rotation, and shear transformation—were applied to simulate real-world variations, resulting in a final training set of 5,768 images. This multi-stage augmentation aimed to improve the model's generalization and robustness.

MobileNet, that have been trained on the ImageNet dataset, is used as the base model. The final layer of the model is adapted for the task of classification of pressure wounds by adding multiple layers to match the output of the classification results, as well as to reduce overfitting. Some of these layers include:

1. Global Average Pooling 2D

Global Average Pooling 2D (GAP 2D) is a layer used in the CNN model to reduce the data dimensions from the previous convolutional layer by calculating the average of each map feature. 2D GAP converts each map feature into a single average value, which reduces the number of parameters in the model, reduces the risk of overfitting,

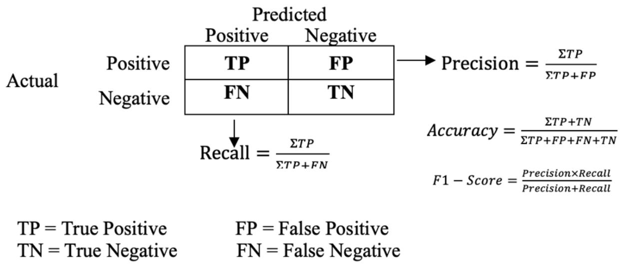

Figure 7. Accuracy, precision, recall, and F1-score formula

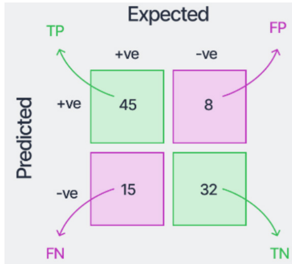

Figure 8. Confusion matrix example

and improves computational efficiency. In addition, 2D GAP provides spatial invariance, which means the model becomes more resistant to changes in the position of objects in the image.

2. Batch Normalization

Batch normalization is a normalization technique applied to the input of the previous layer by calculating the mean and variance of the mini-batch and then normalizing it. Batch normalization helps stabilize and speed up the training process by reducing internal covariate shifts. In addition, it also has a regularizing effect that helps reduce overfitting and allows for the use of higher learning rates as the distribution of activations becomes more stable.

3. Dropout

Dropout is a regularization technique in which several number of neurons in a layer are randomly selected to be disabled during training. This prevents the neuron from becoming overly dependent on a particular neuron, forcing the model to learn more robust representations. The dropout in the model's architecture is set to 40%, which will help in reducing overfitting by adding noise to the training process, making the model more general on new data.

4. Softmax

Softmax layer is the output layer used in classification problems to convert the raw score (logits) of the previous layer into interpretable probabilities. Softmax converts those values into probability distributions by adding up the exponential values of the logits and dividing them by the total sum of those exponents. The result is a probability vector that totals one, with each element representing the probability of each class. The softmax layer allows the model to make predictions that can be interpreted as the probabilities of each class in a multiclass classification problem.

D. Model Testing Procedure

After the training is complete, the model is tested on a separate test set to assess the final performance. Test sets are not used during training or validation, thus providing an indication of the extent to which the model can generalize to new and previously unseen data. Model testing is made to focus on the performance and accuracy of the model in making predictions for each existing class. Testing is carried out using three commonly used methods to evaluate the performance of classification models, namely:

1. Model Accuracy

Accuracy measures the extent to which a model's predictions match the actual labels of the data. This is the simplest metric and is often used to evaluate model performance.

2. Precision, Recall, dan F1-Score

Precision measures how accurately the model predicts positive classes. This is the ratio of correct predictions for a particular class compared to the total predictions for that class. Recall measures how well the model captures all positive examples. This is the ratio of correct predictions for positive classes compared to the total number of actual positive examples.

F1-score can be calculated from the results of precision and recall. F1-score is a harmonic average of precision and recall, providing a balance between the two. This is a useful metric when you need a balance between precision and recall. All formula regarding accuracy, precision, recall, and F1-score is shown in Figure 7.

E. Confusion Matrix

The confusion matrix is a table that shows the number of correct and incorrect predictions for each class. It provides a better understanding of the types of errors made by the model. A confusion matrix example is shown in Figure 8. The term in the confusion matrix could be defined as TP: True Positives (the number of correct predictions for the positive class), FP: False Positives (the number of incorrect predictions for the positive class), TN: True Negatives (the number of correct predictions for the negative class), and FN: False Negatives (the number of correct predictions for the negative class). All these test calculation methods were done automatically using the Python programming language using several important libraries such as TensorFlow, Keras, and Scikit-learn.

III. Results and Discussion

A. Device System Integration

All components of the pressure injury stage classification device were arranged based on the wiring schematics in Figure 2. Figure 9 shows the arrangement of

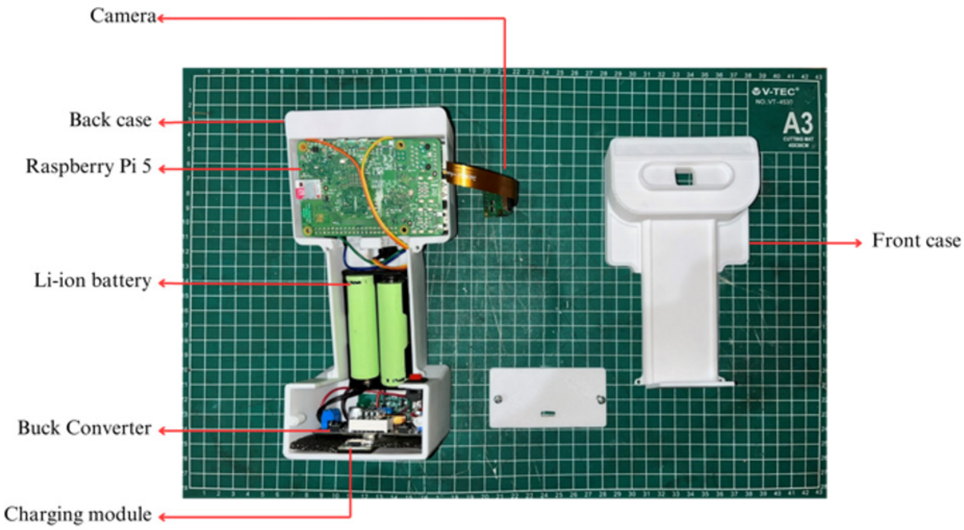

Figure 9. Arrangement of components inside the case of pressure injury stage classification device

(a) (b)

Figure 10. The pressure injury stage classification device: (a) front view; and (b) side view

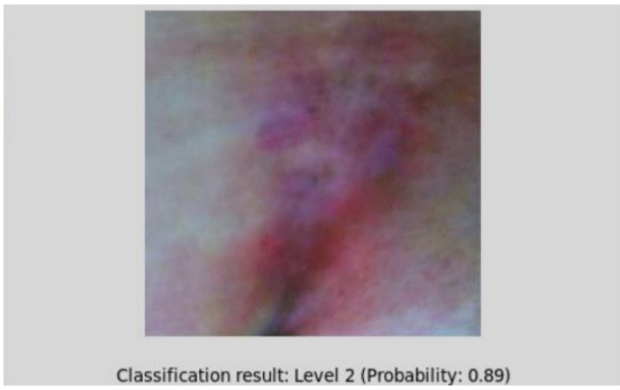

Figure 11. Example of the classification result displayed by the interface

the components inside the case. Figure 10 shows the front and side views of the final product of the system.

Before the integration of the system, each sub-system of the device, both the hardware and software parts, was tested individually to ensure proper functionality. The sub-system of the device is divided into:

1. User Interface

The user interface of the device was built using Tkinter. The testing of this part was conducted to ensure that the interface can function properly and can be easily used by the user. The testing result shows that the real-time display of the camera feed was able to display the appearance of the classification result clearly and accurately. Figure 11 shows an example of the classification result displayed by the interface from real-time image capture. This image was cropped and zoomed to provide image clarity.

2. Power Supply

The power supply test was carried out to verify the stability of the battery in providing power to the components. The result shows that the Li-Ion 18650 battery could supply a maximum of 7.6 V to the microcomputer at 100% SoC, with a stable flow of current at 0.907 A. From this measurement, it is yielded that the device could last 1.4 hours before the battery runs out.

3. Classification Model

The classification model was tested for each stage from stage 1 to 4. The results of each stage are shown in Table 5. It can be clearly seen that the model has a high precision value in all stages; however, quite a significant recall difference was shown in stage 3 and 4. The lowest recall value is at stage 3, indicating difficulty in detecting images in stage 3. In contrast, the recall for Level 4 was excellent, reaching 0.96. The F1-score shows a balance between precision and recall in almost all stages, but it is low again at stage 3. With a total accuracy of 84%, the model performs well, but improvements are needed for the stage 3 class through architectural adjustments or data augmentation.

Figure 12 shows the confusion matrix of the testing classification model. The model performs quite well, with many correct predictions along the diagonal of the confusion matrix. From the total data of 206, the model accuracy is 84%. Specifically, there are 38 correct predictions for stage 1, 53 for stage 2, 39 for stage 3, and 43 for stage 4. However, there are several classification errors that need to be noted. The most prediction errors occurred at stage 3, where 7 images were predicted as stage 2, and 8 images were predicted as stage 4. This shows that

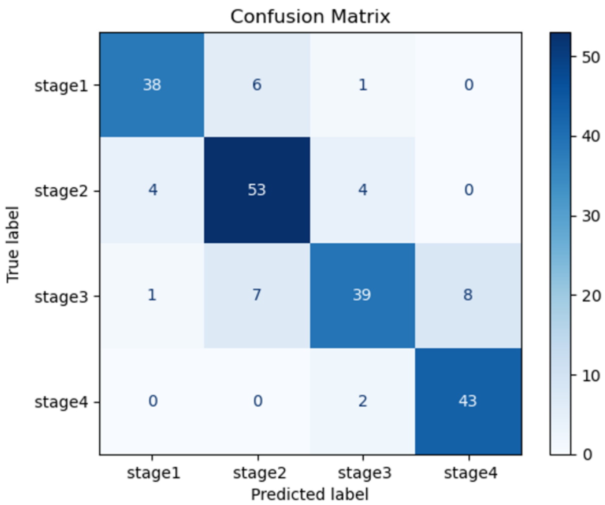

Figure 12. Model classification confusion matrix

Table 5. Classification model report

	Precision	Recall	F1-score	Number of data
Stage 1	0.88	0.87	0.86	45
Stage 2	0.80	0.87	0.83	61
Stage 3	0.84	0.71	0.77	55
Stage 4	0.84	0.96	0.90	45

the model has difficulty predicting stage 3, which is often predicted as stage 2 or 4.

The results of the system integration test show that all components work together harmoniously in one integrated unit. The Raspberry Pi Cam V3 camera is capable of capturing images with vivid and accurate details in a wide range of lighting conditions, meeting the standards required for further processing. The Raspberry Pi 5 processor demonstrates high efficiency in processing images and runs the TFLite model, without significant delays, ensuring that classification results can be provided in real time. The power supply system, consisting of two 18650 Li-ion batteries, a buck converter, and a BMS charger, proved to be stable and efficient, providing enough power for the operation of the entire system for a duration that met expectations (maximum 1.40 hours per cycle). The user interface built using Tkinter works well, displays the camera feed in real-time and classification results clearly, and is easy to use. The model test showed high classification accuracy with minimal error rates, confirming that the TFLite model can classify pressure injury precisely. Overall, the results of the system integration tests show that all components are working well simultaneously, ensuring the system is ready for use in real-world applications and meets the desired specifications.

B. Device Performance Testing

After the system integration, the performance of the device in classifying the stage of pressure injury was tested. Several pressure injury sample images outside the

Table 6. Device performance in pressure injury stage classification

No	Sample image	Classification result*	Verification	Status
1	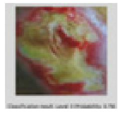	Stage 3	Stage 3	Correct
2	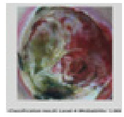	Stage 4	Stage 4	Correct
3	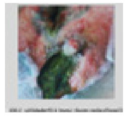	Stage 4	Stage 4	Correct
4	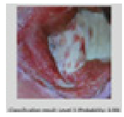	Stage 3	Stage 3	Correct
5	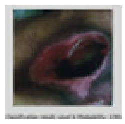	Stage 4	Stage 4	Correct
6		Stage 4	Stage 4	Correct
7	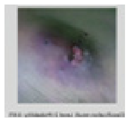	Stage 2	Stage 2	Correct
8		Stage 1	Stage 1	Correct
9	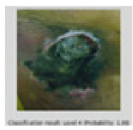	Stage 4	Stage 4	Correct
10		Stage 4	Stage 4	Correct
11	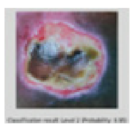	Stage 2	Stage 3	Incorrect
12		Stage 2	Stage 1	Incorrect

dataset were captured using the device camera. All the captured images stages have been verified by a doctor certified in elderly care, as shown in Table 6. However, due to the difficulty in obtaining the real pressure injury subject/ sample, we were not able to use an equal image for each class.

The mean classification duration is 2.24 s, and it could vary due to the process of the camera's focus point determination. The device should be held at the optimal distance of 6-20 cm from the injury (according to the injury/ ulcer size) to achieve better image resolution. Smaller injuries should be captured from a smaller distance to avoid blurriness. On the contrary, bigger injuries should be captured from a higher distance to prevent information loss due to an incomplete image.

Based on the test results, there was a classification error in subject 11, which should have been classified as stage 3, and in subject 12, which should have been classified as stage 1. This error may be due to a lack of depth in a two-dimensional image, which is not capable of depicting the depth of the wound. Furthermore, these misclassifications align with the confusion matrix, which shows several instances where stage 2 images were misclassified as either stage 1 or stage 3. These findings suggest that stage 2 shares overlapping visual characteristics with both stage 1 and stage 3, making accurate classification more challenging for the model.

An overall accuracy value of 83.3% was obtained, with the number of classification results of the correct being 10 out of 12 samples. With this accuracy value, the system is reliable enough to be used in clinical practice. The images and classification stages on each sample have also been verified by experts; however, further improvements may be needed to achieve higher diagnostic standards.

IV. Conclusion

The design and integration of applications and hardware in the pressure injury stage classification device showed satisfactory results, with all key components working harmoniously in one integrated system. The Raspberry Pi Cam V3 camera manages to produce images with clear and accurate detail, while the Raspberry Pi 5 processes images and runs the TFLite model efficiently without significant delays. The stable power supply system and Tkinter's intuitive user interface support the ease of use of the system. The CNN model with MobileNet architecture demonstrates high accuracy (83.3%) in classifying the pressure injury stage, especially for stages 1 and 4. While there are challenges, such as improved accuracy in poor lighting conditions and the need for further validation in clinical scenarios, overall, the system has great potential to improve faster and more accurate pressure injury assessment in clinical settings.

References

[1] R. Chou, T. Dana, C. Bougatsos, I. Blazina, A. J. Starmer, K. Reitel, and D. I. Buckley, "Pressure ulcer risk assessment and prevention: a systematic comparative effectiveness review," *Annals of Internal Medicine*, vol. 159, no. 1, pp. 28-38, Jul 2013.

[2] S. Gaspar, M. Peralta, A. Marques, A. Budri, M. Gaspar de Matos, "Effectiveness on hospital-acquired pressure ulcers prevention: a systematic review," *Int Wound J,* vol. 16, no. 5, pp. 1087-1102, Oct 2019.

[3] H. Yousef, M. Alhajj, and S. Sharma, *Anatomy, Skin (Integument), Epidermis*. Treasure Island, FL: StatPearls Publishing, 2024.

[4] R. G. Kessel, *Basic Medical Histology: The Biology of Cells, Tissues, and Organs*. New York, USA: Oxford University Press, 1999.

[5] J. Y. Kim, Y. J. Lee, and Korean Association of Wound Ostomy Continence Nurses, "Medical device-related pressure ulcer (MDRPU) in acute care hospitals and its perceived importance and prevention performance by clinical nurses," *Int Wound J.*, vol.16, pp. 51-61, Mar 2019.

[6] Y. Sari, A. S. Upoyo, A. Sumeru, W. A. Mulyono, and A. Anam, "Nurses' perceived barriers to the prevention of pressure injury and related factors in Indonesia," *J Bionursing*, vol. 5, no. 2, pp. 119-127, May 2023.

[7] N. F. Mamoto and J. Gessal, "Rehabilitasi medik pada pasien geriatri ulkus decubitus," *J Medik dan Rehabilitasi*, vol. 1, no. 1, pp. 32-37, Sep 2018.

[8] S. N. Yusharyahya, L. Legiawati, R. Astriningrum, R. Jonlean, and V. Andhira, "Characteristics of pressure injuries among geriatric patients at an Indonesian tertiary hospital: A cross-sectional study," *Medical J Indonesia*, vol. 32, no. 3, pp. 183-189, Nov 2023.

[9] NPIAP, Pressure Injury Stages, National Pressure Ulcer Advisory Panel, 2016. [Online]. Available: https://npiap.com/page/PressureInjuryStages. [Accessed: Aug. 18, 2024].

[10] E. D. Kale, E. Nurachmah, and H. Pujasari, "Penggunaan skala braden terbukti efektif dalam memprediksi kejadian luka tekan," *Jurnal Keperawatan Indonesia*, vol. 17, no. 3, pp. 95-100, Feb 2014.

[11] M. Yip, D. Da He, E. S. Winokur, A. G. Balderrama, R. L. Sheridan, and H. Ma, "A flexible pressure monitoring system for pressure ulcer prevention," in Proc. 31st Annual Int. Conf. IEEE Eng. Med. Biol. Soc. (EMBC), 2009, pp. 1212–1215.

[12] T. V. Boyko, M. T. Longaker, and G. P. Yang, "Review of the current management of pressure ulcers," *Adv Wound Care (New Rochelle)*, vol. 7, no. 2, pp. 57-67. Feb 2018.

[13] M. H. Hilmi, "Identifikasi luka tekan pada lansia menggunakan sensor warna," B.Eng. Thesis, Telkom University, 2022.

[14] R. H. L. Silva and A. M. C. Machado, "Automatic measurement of pressure ulcers using support vector machines and GrabCut," *Comput Methods Programs Biomed*, vol. 200, pp. 105867, 2021.

[15] E. Kwong and G. Pang, "Development of an intelligent seat for the alleviation of pressure ulcers," in Proc. 2018 11th Biomedical Engineering International Conference (BMEiCON), 2018, pp. 1-5.

[16] M. Swerdlow, O. Guler, R. Yaakov, and D. G. Armstrong, "Simultaneous segmentation and classification of pressure injury image data using mask-R-CNN," *Comput Math Methods Med*, vol. 2023, p. 3858997, 2023.

[17] S. Zaha, B. Garcia-Zapirain, and A. Elmaghraby, "Integrating 3D model representation for an accurate non-invasive assessment of pressure injuries with deep learning," *Sensors*, vol. 20, no. 10, p. 2933, May 2020.

[18] F. J. Veredas, H. Mesa, and L. Morente, "Efficient detection of wound bed and peripheral skin with statistical colour models," *Med Biol Eng Comput*, vol. 53, no. 4, pp. 345-59, Apr 2015.

[19] K. O'Shea and R. Nash, "An introduction to Convolutional

Neural Networks," *Neural Evolutionary Comput*., Nov. 2015, [Online]. Available: https://doi.org/10.48550/arXiv.1511.08458. [Accessed: Aug. 18, 2024].

[20] J. Wu, *Introduction to Convolutional Neural Networks*, LAMBDA Group, National Key Lab for Novel Software Technology, Nanjing University: China, p. 495, May 2017

[21] S. Bunrit, N. Kerdprasop, and K. Kerdprasop, "Evaluating on the transfer learning of CNN architectures to a construction material image classification task," *Int J Mach Learn Comput*, vol. 9, no. 2, pp. 201-207, Apr 2019.

[22] A. G. Howard et al., "MobileNets: efficient Convolutional Neural Networks for Mobile Vision applications," *Neural Evolutionary Comput*, Apr. 2017, [Online]. Available: https://doi.org/10.48550/arXiv.1704.04861. [Accessed: Aug. 18, 2024].

[23] X. Li, M. Cen, J. Xu, H. Zhang, and X. S. Xu, "Improving feature extraction from histopathological images through a fine-tuning ImageNet model," *J Pathol Inform*, vol. 13, Jan 2022.

[24] Roboflow, Pressure Wounds V11 Computer Vision Project. [Online]. Available: https://universe.roboflow.com/thsbcs2/pressure-wounds-v11. [Accessed: Aug. 18, 2024].